



# PHOTONICS Research

## Quantum dot mode-locked frequency comb with ultra-stable 25.5 GHz spacing between 20°C and 120°C

SHUJIE PAN,<sup>1,†</sup> JIANOU HUANG,<sup>2,†</sup> ZICHUAN ZHOU,<sup>1</sup> ZHIXIN LIU,<sup>1</sup>  LALITHA PONNAMPALAM,<sup>1</sup>  ZIZHUO LIU,<sup>1</sup> MINGCHU TANG,<sup>1</sup> MU-CHIEH LO,<sup>1</sup>  ZIZHENG CAO,<sup>2,5</sup> KENICHI NISHI,<sup>3</sup> KEIZO TAKEMASA,<sup>3</sup> MITSURU SUGAWARA,<sup>3</sup> RICHARD PENTY,<sup>4</sup> IAN WHITE,<sup>4</sup> ALWYN SEEDS,<sup>1</sup> HUIYUN LIU,<sup>1</sup> AND SIMING CHEN<sup>1,\*</sup>

<sup>1</sup>Department of Electronic and Electrical Engineering, University College London, Torrington Place, London, WC1E 7JE, United Kingdom

<sup>2</sup>Institute of Photonic Integration, Eindhoven University of Technology, Eindhoven 5600 MB, The Netherlands

<sup>3</sup>QD Laser, Inc., Kawasaki 210-0855, Japan

<sup>4</sup>Centre for Photonics Systems, Department of Engineering, University of Cambridge, Cambridge CB3 0FA, United Kingdom

<sup>5</sup>e-mail: z.cao@tue.nl

\*Corresponding author: siming.chen@ucl.ac.uk

Received 10 June 2020; revised 2 September 2020; accepted 14 September 2020; posted 18 September 2020 (Doc. ID 399957); published 30 November 2020

Semiconductor mode-locked lasers (MLLs) are promising frequency comb sources for dense wavelength-division-multiplexing (DWDM) data communications. Practical data communication requires a frequency-stable comb source in a temperature-varying environment and a minimum tone spacing of 25 GHz to support high-speed DWDM transmissions. To the best of our knowledge, however, to date, there have been no demonstrations of comb sources that simultaneously offer a high repetition rate and stable mode spacing over an ultrawide temperature range. Here, we report a frequency comb source based on a quantum dot (QD) MLL that generates a frequency comb with stable mode spacing over an ultrabroad temperature range of 20–120°C. The two-section passively mode-locked InAs QD MLL comb source produces an ultra-stable fundamental repetition rate of 25.5 GHz (corresponding to a 25.5 GHz spacing between adjacent tones in the frequency domain) with a variation of 0.07 GHz in the tone spacing over the tested temperature range. By keeping the saturable absorber reversely biased at  $-2$  V, stable mode-locking over the whole temperature range can be achieved by tuning the current of the gain section only, providing easy control of the device. At an elevated temperature of 100°C, the device shows a 6 dB comb bandwidth of 4.81 nm and 31 tones with  $>36$  dB optical signal-to-noise ratio. The corresponding relative intensity noise, averaged between 0.5 GHz and 10 GHz, is  $-146$  dBc/Hz. Our results show the viability of the InAs QD MLLs as ultra-stable, uncooled frequency comb sources for low-cost, large-bandwidth, and low-energy-consumption optical data communications.

Published by Chinese Laser Press under the terms of the [Creative Commons Attribution 4.0 License](https://creativecommons.org/licenses/by/4.0/). Further distribution of this work must maintain attribution to the author(s) and the published article's title, journal citation, and DOI.

<https://doi.org/10.1364/PRJ.399957>

### 1. INTRODUCTION

Optical frequency combs consisting of equally spaced discrete optical frequency components have emerged as promising tools for a wide range of applications including metrology, optical communications, optical clock distribution/recovery, radio-over-fiber signal generation, and optical sampling [1–7]. Integrated comb sources are particularly attractive due to the size and power consumption advantages and are being heavily investigated as light sources for short and medium reach dense wavelength-division multiplexing (DWDM) communications systems [2,4]. For instance, a microring-resonator-based Kerr

frequency comb has been used to demonstrate C+L band coherent communications with  $>30$  Tbit/s (terabits per second) data rate [2]. However, practical systems also require a comb source to work stably over a wide temperature range (e.g.,  $-20^\circ\text{C}$  to  $85^\circ\text{C}$ ).

A semiconductor mode-locked laser (MLL) represents a simple and low-cost approach to generate frequency combs. Short-cavity MLLs can generate high repetition rate (thus, large tone spacing) and high optical signal-to-noise ratio (OSNR) frequency combs that suit DWDM communications. An MLL typically provides 5–10 nm bandwidth, promising

comb-based transmitters [8]. The recent development of quantum dot (QD) semiconductor material promises an ultrabroad gain bandwidth and ultrafast carrier dynamics [9], with many other important features including large gain and saturable absorber (SA) saturation energy ratio [10], low spontaneous emission rate [11], and the capability for monolithic integration with silicon substrates [12–15]. These promising features have inspired much research in the development of high-performance QD MLLs [16–21] and their applications for multi Tbit/s communications [22–26].

Temperature resilience has long been the hallmark of QDs, due mainly to their delta-function-like density of states [27]. While high-temperature continuous-wave (CW) operation up to 220°C from InAs QD Fabry–Perot (FP) lasers has been demonstrated [28], exclusively from the QD ground state (GS) transition, turning this prediction into reality for QD MLLs involves not only thermal mechanisms but also the mutual interdependence of the gain section and the SA in two-section passive devices. The work of Cataluna *et al.* first emphasized the stability of mode-locking in 20 GHz InGaAs QD MLLs at elevated temperatures. However, the device exhibited unstable mode-locking operation over 70°C evidenced by radio-frequency (RF) SNR quenching (15 dB at 80°C) [29]. Stable mode-locking, exclusively through GS transition, from 20°C to 92°C, has also been demonstrated from two-section passive InAs QD MLLs [30]. However, mode-locking switching between GS and the first excited state (ES1) appears due to the carrier escape from the GS with increasing temperature, and the long laser cavity of 8 mm employed in their work limited the fundamental repetition rate to 5 GHz, which is not high enough to meet the minimum requirement (e.g., 25 GHz) of DWDM systems.

Although one may expect a broad mode-locking temperature range from one QD mode-locked device [29,30] and observe a large mode spacing from another [31], a key challenge is to achieve simultaneously ultra-stable mode spacing over an extremely broad temperature range from a single frequency comb light source with large mode spacing. In this paper, by developing a QD active region with high dot density and large energy separation between the GS and higher energy states, we demonstrate stable mode-locking operating over a record temperature range between 20°C and 120°C. Our QD MLL operates at the telecom O band and exhibits coherent optical pulses at a repetition rate of 25.5 GHz, and correspondingly, 25.5 GHz spacing between adjacent tones in the frequency domain. With temperature increased from 20°C to 120°C, the tone spacing changes by only approximately 0.07 GHz. Moreover, our device emits a comb bandwidth of 4.81 nm at an operating temperature of 100°C with 31 total channels within the 6 dB comb bandwidth. The corresponding average relative intensity noise (RIN) for the whole lasing spectrum was measured to be  $-146$  dBc/Hz in the frequency range from 0.5 GHz (due to the limitation of the equipment) to 10 GHz. The demonstrated performance suggests the developed QD MLL is a strong candidate for an ultra-stable, uncooled frequency comb light source that can be employed in a low-cost optical network system with high capacity and efficiency.

## 2. MATERIAL AND DEVICE DESIGN

The InAs QD laser structure was grown on a Si-doped GaAs (001) substrate using molecular beam epitaxy (MBE). The epitaxy starts with a 300 nm thick n-type GaAs buffer layer followed by a combination of n-type  $\text{Al}_{0.2}\text{Ga}_{0.8}\text{As}/\text{Al}_{0.4}\text{Ga}_{0.6}\text{As}/\text{Al}_{0.2}\text{Ga}_{0.8}\text{As}$  in a thickness of 200 nm/1400 nm/200 nm, which acts as the lower cladding layer. Above the lower cladding layer is the active region, followed by another combination of  $\text{Al}_{0.2}\text{Ga}_{0.8}\text{As}/\text{Al}_{0.4}\text{Ga}_{0.6}\text{As}/\text{Al}_{0.2}\text{Ga}_{0.8}\text{As}$  p-type upper cladding layer in a thickness of 200 nm/1400 nm/200 nm, respectively, and finally a 300 nm highly p-doped GaAs contact layer. A high optical gain is always desired for high-temperature operation of QD lasers; here, to this end, a larger than usual number of QD layers, with higher dot area density, were employed for the QD active region. For the growth of the active region, without adopting a conventional InAs/InGaAs/GaAs dot-in-a-well (DWELL) structure, where the InAs layer is sandwiched by InGaAs layers, here, InAs QDs were formed self-assembly on a GaAs surface by depositing a three-monolayer InAs QD layer directly on the GaAs surface. The initial InAs QDs were then covered by a 3.7 nm InGaAs strain-reducing layer (SRL), and such coverage growth conditions were also optimized to suppress ad-atom migration during the coverage. By doing so, the original uniformity can be kept without sacrificing dot density and multilayer structures. This could result in rather narrow photoluminescence (PL) emission from those QDs. Figure 1(a) illustrates the cross-sectional transmission electron microscopy (TEM) image of the active region presented in this paper, comprising a tenfold layer stack of InAs QDs (twice the number of layers previously used in Ref. [12]). From the high-resolution bright-field scanning TEM image of a single dot, as shown in the inset of Fig. 1(a), the typical dot size is  $\sim 20$  nm in diameter and  $\sim 7$  nm

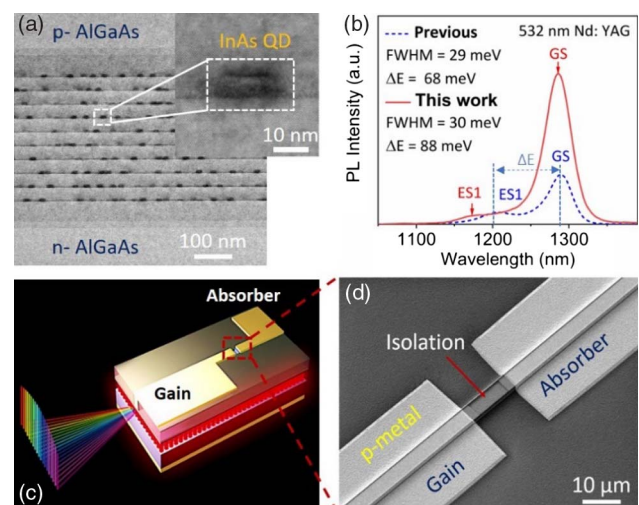


**Fig. 1.** (a) Cross-sectional TEM image of the active region. The inset shows the high-resolution bright-field scanning TEM image of a single dot. (b) Comparison of the room temperature PL spectra for samples grown under previous conditions and the optimized growth conditions employed in this work. (c) Schematic of the passive two-section MLL. (d) SEM image of the device showing the gap between the gain and SA.

in height. Dot density as high as  $5.9 \times 10^{10} \text{ cm}^{-2}$  is typically obtained in these structures [32] (nearly double the previous dot density of  $3 \times 10^{10} \text{ cm}^{-2}$ ). Figure 1(b) compares the room temperature PL spectra for the full QD laser epi wafer grown under previous conditions and the optimized growth condition, which has been employed in this work. As seen, despite the high dot density that was achieved, the PL full width at half maximum (FWHM) (governed by the inhomogeneous broadening due to size and shape distribution of the QDs) remained as low as 30 meV, which is comparable to our previous observation of 29 meV with low dot density. The combined effects have led to an enhancement of integrated PL intensity of the optimized sample at 2.6 times higher than the previous one. In addition, the quantized-energy difference ( $\Delta E$ ) between the GS and ES1 increased from 68 meV to 88 meV. The enhanced energy separation plays a vital role in effectively suppressing the carrier overflow and Auger recombination at elevated temperatures [28].

The MLLs were fabricated from the wafer described above following standard etching and metal–dielectric deposition techniques. Figure 1(c) shows a schematic diagram of the fabricated MLL. As can be seen, the device has a typical two-section ridge-waveguide laser structure with a 15  $\mu\text{m}$  gap in the top p-type contact metals, and the ridge width is 5  $\mu\text{m}$ . To achieve a fundamental repetition rate of 25 GHz, the total length of the laser investigated in this paper was set to be 1615  $\mu\text{m}$  with the length of the absorber designed to be 200  $\mu\text{m}$ , corresponding to a gain-to-absorber length ratio of 7:1. The isolation between the gain section and the absorber section is achieved by using shallow wet etching to selectively remove the heavily p-doped contact layer in the gap region, as indicated in Fig. 1(d). The measured isolation resistance is 8 k $\Omega$ . No coating is applied to the cleaved facets. The devices were mounted p-side up on an indium-plated copper heat sink and gold-wire-bonded to enable testing.

### 3. RESULT AND DISCUSSION

CW performance of the fabricated InAs QD MLL comb source was first characterized at room temperature, as shown in Fig. 2. Figure 2(a) shows typical light-current ( $L-I$ ) characteristics at various reverse-bias voltages. As seen, while the  $L-I$  characteristics did not reveal pronounced hysteresis on the device under investigation, the nonlinear saturation effect of the SA can be observed for the higher reverse-bias voltages evidenced by the sudden power rise near the threshold. Incrementing the reverse-bias voltage caused a threshold increase from 17 mA to 29 mA due to the enhanced absorption loss within the SA region, which, as would be expected, also leads to decreased slope efficiency. The range of driving conditions over which stable mode-locking occurs in this device is illustrated in Fig. 2(b). In this work, a stable mode-locking state was defined as a fundamental frequency tone SNR of over 25 dB [resolution bandwidth (RBW): 1 MHz, video bandwidth (VBW): 10 kHz] and the corresponding pulse width narrower than 15 ps. Here, although the device configuration of a high gain-to-absorption ratio of 7:1 was employed, stable mode-locking over a wide range of drive currents ranging from 30 mA to 115 mA and reverse-bias voltages from 1.5 V to 7 V was demonstrated. A wider range of mode-locking driving conditions could be

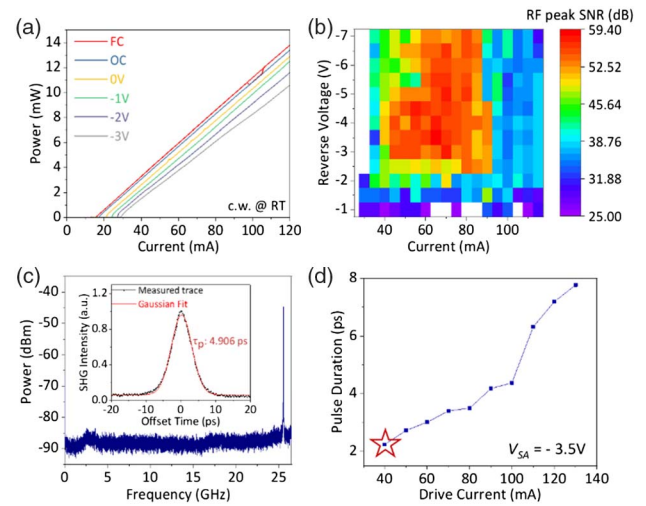


**Fig. 2.** Two-section passive QD-MLL performance characterization at room temperature. (a)  $L-I$  characteristics for different SA reverse-bias voltages. (b) Fundamental RF peak SNR mapping. (c) RF spectrum in a 26.5 GHz span view (RBW: 1 MHz, VBW: 10 kHz). The inset shows the autocorrelation trace with Gaussian pulse fitting. (d) Pulse duration as a function of  $I_{\text{gain}}$  with  $V_{\text{SA}} = -3.5 \text{ V}$ .

achieved by employing device configurations with lower gain-to-absorption ratios [10,33].

Figure 2(c) depicts a representative RF trace for the bias conditions of  $I_{\text{gain}} = 75.22 \text{ mA}$  and  $V_{\text{SA}} = -2.9 \text{ V}$ . A narrow linewidth fundamental RF tone at 25.54 GHz with an SNR of 47.9 dB is clearly indicated, corresponding to the free spectral range of our device. The absence of low-frequency fluctuations or  $Q$ -switched mode-locking is also noted. The corresponding autocorrelation trace is displayed in the inset of Fig. 2(c). A pulse duration of 4.906 ps was obtained, assuming a Gaussian pulse profile. Shorter pulse durations were observed from the same device at lower driving currents and higher reverse-bias voltages, as shown in Fig. 2(d), where the narrowest pulse of 2.23 ps was achieved under the bias conditions of  $I_{\text{gain}} = 40 \text{ mA}$  and  $V_{\text{SA}} = -3.5 \text{ V}$ . The pulse duration is expected to be further shortened by decreasing the gain-to-absorption ratio through more effective shaping dynamics within the QD material [10].

The effect of temperature on the  $L-I$  characteristics, when the reverse-bias voltage was fixed at 0 V, is presented in Fig. 3(a) for the same device as illustrated in Fig. 2. CW lasing was maintained until the testing was stopped at a heatsink temperature of 120°C due to the limitation of the test system. Under these conditions, no thermal rollover behavior was observed. Figure 3(b) highlights the effect of changes in the temperature and SA reverse-bias voltage on the threshold current. While, at a fixed reverse-bias voltage, for an increase in the temperature, the threshold current is generally increased, the calculated characteristic temperature  $T_0$  remains an almost consistent value of around 55 K with reverse-bias voltage, indicating that  $T_0$  is ultimately related to the physical properties of the gain section. This observation has also been previously observed in two-section quantum-well as well as QD lasers [34]. It is also noted that the modulation of loss in the SA by the reverse-bias voltage

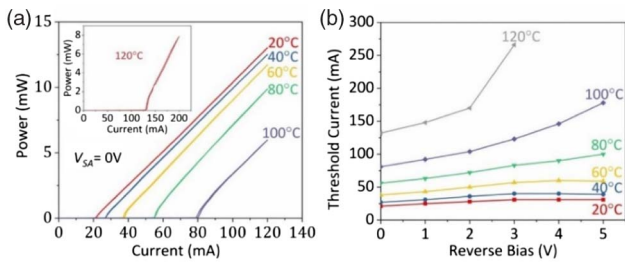


**Fig. 3.** (a) Typical CW  $L-I$  characteristics of the two-section QD MLL as a function of temperature when  $V_{SA} = 0$  V. (b) Dependence of threshold current on reverse-bias voltage and temperature.

was more prominent for high temperatures, which was evidenced by the subtle hysteresis loops observed when the temperature exceeded 60°C.

To evaluate the temperature performance of our QD MLL comb source, RF spectra were first measured as a function of temperature at a fixed reverse-bias voltage of 2 V, as shown in Fig. 4(a). The driving currents were 49, 60, 64.7, 85, 148.5, and 210 mA at 20, 40, 60, 80, 100, and 120°C, respectively, chosen because it produces the shortest pulse width at the given temperature. Stable mode-locking operation over an extended temperature range from 20°C to 120°C has been achieved, with the SNR well over 30 dB and the corresponding pulse width narrower than 9 ps presented in Fig. 4(c). To the best of our knowledge, this is the broadest mode-locking operation temperature range ever reported to date for any type of MLL. It was of significance, observed in Fig. 4(b), that the change in mode spacing was only 0.07 GHz over the extremely broad temperature range of 100°C. Typically, an increase in the temperature leads to thermal expansion of the cavity length, and

subsequently, a reduction in the tone spacing. However, as the temperature increases, the reduced refractive index of the semiconductor for a given wavelength results in an increase in the tone spacing. For the results presented, the effect of temperature on thermal expansion of the laser and the change of refractive index is well balanced, and thus the tone spacing remains ultra-stable with temperature, which is a desirable feature for optical communications. Furthermore, given that the temperature-dependent operation of a passive two-section MLL involves a mutual interplay of the gain section and the SA, here, for the device presented, with the SA reversed biased at a constant voltage, stable mode-locking over an ultrabroad temperature range has been easily achieved by simply adjusting the electrical biasing conditions, which yields an added benefit of bias simplicity.

The pulse duration change over temperature is presented in Fig. 4(c); as seen, the value ranges from  $\sim 5$  ps to  $\sim 8$  ps between 20°C and 120°C. Note that the pulse duration presented here indicates the shortest pulse width that can be achieved at the given temperature. By carefully optimizing the driving conditions at each temperature, a relatively stable pulse duration of  $\sim 8$  ps over the entire temperature range between 20°C and 120°C could be achieved. Figure 4(d) shows a color contour map depicting the regions of fundamental mode-locking (25.5 GHz) from 20°C to 120°C where the measured SNR of the RF tone is larger than 25 dB. It is worth mentioning that the range of driving conditions for expected stable mode-locking at each temperature should be broader than indicated since the testing range employed was underestimated [35]. Even so, it is quite apparent that an achievable mode-locking range shrinks as the temperature increases.

QD MLLs that operate at the GS are of interest in the context of optical communication systems owing to the desirable

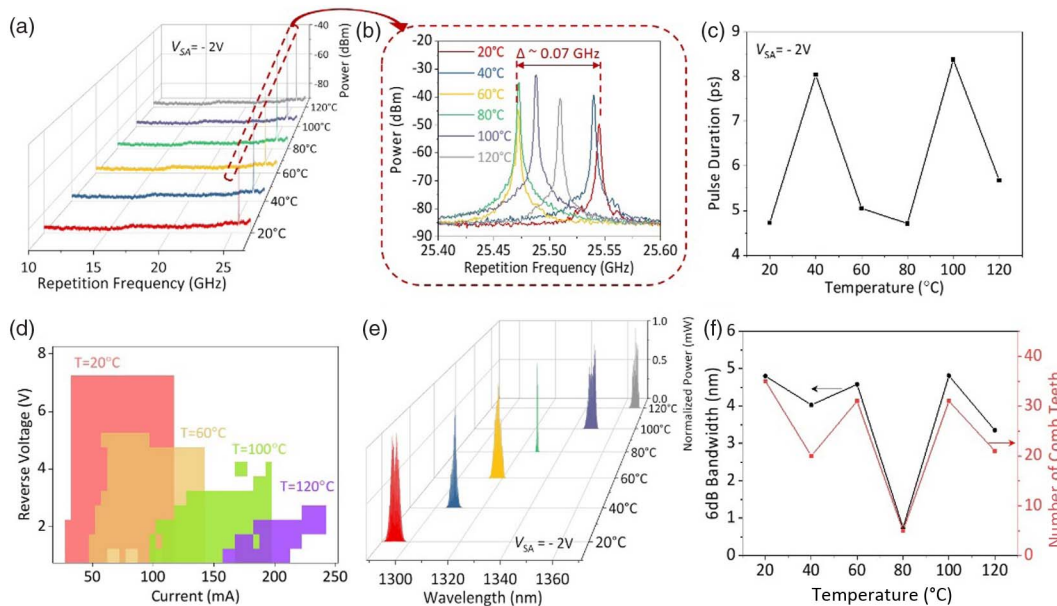


**Fig. 4.** Temperature-dependent characteristics of two-section passive QD-MLL with a constant  $V_{SA} = -2$  V and  $I_{gain}$  of 49, 60, 64.7, 85, 148.5, and 210 mA at 20, 40, 60, 80, 100, and 120°C, respectively. (a) RF spectra (RBW: 1 MHz, VBW: 10 kHz). (b) Zoomed-in RF spectra, as shown in (a). (c) Pulse duration. (d) Color map depicting the regions of fundamental mode-locking (25 GHz) from 20°C to 120°C where the SNR > 25 dB. (e) Optical spectra (resolution: 0.03 nm, VBW: 200 Hz). (f) 6 dB bandwidth and the corresponding number of comb teeth.

features of low power consumption and high wall-plug efficiency. However, operation at higher temperatures may shift the emission to the ES1 because of their lower gain and the relatively small quantized energy separation between the GS and the ES1. It was also thought that this phenomenon occurs more notably for those in shorter cavity QD MLLs with higher repetition rates. In this work, mode-locking exclusively from the GS has been achieved over the entire temperature range from 20°C to 120°C, evidenced by the measured optical spectra as a function of temperature shown in Fig. 4(e). It is noted that the absolute wavelengths of the MLL are indeed changing versus their operating temperature ( $\sim 0.7$  nm/°C), which is an undesirable feature for practical comb applications. However, by carefully tailoring the QD structure as well as the laser cavity length, i.e., achieving an optimum cavity design for a given gain function [36], this thermal-induced red shift could be dramatically restricted. Therefore, it would be possible to obtain a stable mode-locked QD comb source with an extremely low change in the wavelength of each comb line with temperature. Nevertheless, the small change of tone spacing achieved in this paper promises a small guardband between adjacent DWDM channels [8], ensuring high spectral efficiency for multi-Tbit/s interconnects. Figure 4(f) summarizes the optical spectrum flatness at each temperature under the same driving condition as in Fig. 4(e). As seen, the 6 dB comb bandwidth for most of the conditions is relatively constant within the range of 3.5 nm to 4.7 nm, and it is interesting to observe a very narrow comb bandwidth at 80°C. This phenomenon is still under investigation and possibly related to a combined effect of the cavity design, driving condition, and temperature-dependent tuning of the gain and absorption magnitude at the lasing wavelength. Further improvement of the comb bandwidth could be achieved by using chirped QDs [37], QD intermixing [38], and hybrid quantum well/QD structures [39]. Also, as expected, the corresponding number of comb teeth as a function of temperature shows a similar trend as the comb bandwidth. As seen, even at 120°C, it can still obtain  $>20$  comb lines.

To evaluate the suitability of the developed QD MLL employed as an uncooled frequency comb light source for DWDM optical commutations, the comb spectrum and the RIN were characterized at a high temperature of 100°C. Figure 5(a) shows the coherent comb spectrum, which exhibits a center lasing wavelength of  $\sim 1349$  nm and a 6 dB comb bandwidth of 4.81 nm (under the bias conditions of  $I_{\text{gain}} = 148.5$  mA and  $V_{\text{SA}} = -2$  V), providing a maximum of 31 potential channels with an OSNR of more than 36 dB [0.1 nm amplified spontaneous emission (ASE) noise bandwidth]. Figure 5(b) shows the RIN spectrum in the frequency range from 0.5 GHz to 10 GHz, where a low average RIN value of less than  $-146$  dBc/Hz was achieved. The measured average absolute power per channel within the 6 dB comb bandwidth is  $\sim -18$  dBm at 100°C, which is comparable to previous observations measured at room temperature [22]. While it is difficult to estimate the actual transmission capacity of this comb laser source at 100°C until a system-level WDM experiment employing an advanced modulation format with direct detection is performed, as a guideline, an anticipated transmission capacity of over 3.4 Tbit/s could be realized by

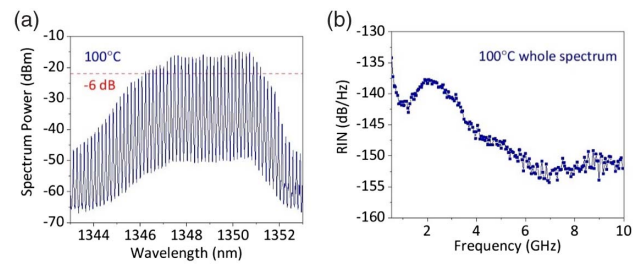


**Fig. 5.** (a) Optical comb under bias conditions of  $I_{\text{gain}} = 148.5$  mA and  $V_{\text{SA}} = -2$  V at 100°C. (b) Average RIN for the whole optical comb shown in (a) from 0.5 to 10 GHz.

employing 31 tones as optical carriers combined with a 28 GBaud pulse amplitude modulation (PAM)-4 format [22,23].

#### 4. CONCLUSION

We have developed a frequency comb source based on a passively mode-locked InAs QD laser that has achieved an ultra-stable repetition rate (corresponding to mode spacing between adjacent tones in the frequency domain) over the widest temperature range yet reported for any type of MLL, due to the high dot density and engineered quantized energy difference between the GS and the ES1. The QD MLL comb source operates at the O band and exhibits stable mode-locking at a fundamental repetition rate of 25 GHz with pulse widths of less than 9 ps at temperatures ranging from 20°C to 120°C. We have shown that the tone frequency spacing is nearly unaltered (0.07 GHz) with increasing operating temperature and that stable mode-locking over a 100°C temperature range can be simply achieved (with the absorber reversed biased at a constant voltage) by changing only the biasing conditions of the gain section. The QD comb source shows a relatively broad, coherent comb bandwidth (with a 6 dB bandwidth of 4.81 nm, offering a maximum of 31 optical channels) at 100°C with a low average RIN value of less than  $-146$  dBc/Hz, making it feasible to handle a multi-Tbit/s transmission capacity. The findings pave the way for utilizing ultra-stable, easy-operating, uncooled QD MLLs as efficient frequency comb sources for high-bandwidth, large-scale, low-cost WDM in optical communications.

**Funding.** Royal Academy of Engineering (RF201617/16/28); Engineering and Physical Sciences Research Council (EP/R041792/1, EP/T01394X/1).

**Acknowledgment.** The authors would like to acknowledge Dr. Mengya Liao and Dr. Kasia Balakier from University College London, and Dr. Wei Li from Beijing University of Technology for performing TEM characterization. S.C. acknowledges the Royal Academy of Engineering for funding his Research Fellowship. S.P. acknowledges the Chinese Scholarship Council for funding her study.

**Disclosures.** The authors declare no conflicts of interest.

<sup>†</sup>These authors contributed equally to this work.

## REFERENCES

- N. Picqué and T. W. Hänsch, "Frequency comb spectroscopy," *Nat. Photonics* **13**, 146–157 (2019).
- P. Marin-Palomo, J. N. Kemal, M. Karpov, A. Kordts, J. Pfeifle, M. H. P. Pfeiffer, P. Trocha, S. Wolf, V. Brasch, M. H. Anderson, R. Rosenberger, K. Vijayan, W. Freude, T. J. Kippenberg, and C. Koos, "Microresonator-based solitons for massively parallel coherent optical communications," *Nature* **546**, 274–279 (2017).
- B. J. Bloom, T. L. Nicholson, J. R. Williams, S. L. Campbell, M. Bishof, X. Zhang, W. Zhang, S. L. Bromley, and J. Ye, "An optical lattice clock with accuracy and stability at the  $10^{-18}$  level," *Nature* **506**, 71–75 (2014).
- L. Lundberg, M. Mazur, A. Mirani, B. Foo, J. Schröder, V. Torres-Company, M. Karlsson, and P. A. Andrekson, "Phase-coherent light-wave communications with frequency combs," *Nat. Commun.* **11**, 201 (2020).
- A. J. Metcalf, H.-J. Kim, D. E. Leaird, A. J. Jaramillo-Villegas, K. A. McKinzie, V. Lal, A. Hosseini, G. E. Hoefler, F. Kish, and A. M. Weiner, "Integrated line-by-line optical pulse shaper for high-fidelity and rapidly reconfigurable RF-filtering," *Opt. Express* **24**, 23925–23940 (2016).
- C. Deakin and Z. Liu, "Dual frequency comb assisted analog-to-digital conversion," *Opt. Lett.* **45**, 173–176 (2020).
- W. Wang, K. V. Gasse, V. Moskalenko, S. Latkowski, E. Bente, B. Kuyken, and G. A. Roelkens, "III-V-on-Si ultra-dense comb laser," *Light: Sci. Appl.* **6**, e16260 (2017).
- Z. Liu, S. Farwell, M. Wale, D. J. Richardson, and R. Slavik, "InP-based optical comb-locked tunable transmitter," in *Optical Fiber Communications Conference and Exhibition (OSA, 2016)*, paper Tu2K.2.
- E. U. Rafailov, M. A. Cataluna, and W. Sibbett, "Mode-locked quantum-dot lasers," *Nat. Photonics* **1**, 395–401 (2007).
- M. G. Thompson, A. R. Rae, M. Xia, R. V. Penty, and I. H. White, "InGaAs quantum-dot mode-locked laser diodes," *IEEE J. Sel. Top. Quantum Electron.* **15**, 661–672 (2009).
- G. Carpintero, M. G. Thompson, R. V. Penty, and I. H. White, "Low noise performance of passively mode-locked 10-GHz quantum-dot laser diode," *IEEE Photon. Technol. Lett.* **21**, 389–391 (2009).
- S. Chen, W. Li, J. Wu, Q. Jiang, M. Tang, S. Shutts, S. N. Elliott, A. Sobiesierski, A. Seeds, I. Ross, P. M. Smowton, and H. Liu, "Electrically pumped continuous-wave III-V quantum dot lasers on silicon," *Nat. Photonics* **10**, 307–311 (2016).
- M. Liao, S. Chen, Z. Liu, Y. Wang, L. Ponnampalam, Z. Zhou, J. Wu, M. Tang, S. Shutts, Z. Liu, P. M. Smowton, S. Yu, A. Seeds, and H. Liu, "Low-noise 1.3  $\mu\text{m}$  InAs/GaAs quantum dot laser monolithically grown on silicon," *Photon. Res.* **6**, 1062–1066 (2018).
- T. Zhou, M. Tang, G. Xiang, B. Xiang, S. Hark, M. Martin, T. Baron, S. Pan, J. Park, Z. Liu, S. Chen, Z. Zhang, and H. Liu, "Continuous-wave quantum dot photonic crystal lasers grown on on-axis Si (001)," *Nat. Commun.* **11**, 977 (2020).
- Z. Liu, C. Hantschmann, M. Tang, Y. Lu, J. Park, M. Liao, S. Pan, A. M. Sanchez, R. Beanland, M. Martin, T. Baron, S. Chen, A. J. Seeds, I. White, R. Penty, and H. Liu, "Origin of defect tolerance in InAs/GaAs quantum dot lasers grown on silicon," *J. Lightwave Technol.* **38**, 240–248 (2020).
- F. Kefelian, S. O'Donoghue, M. T. Todaro, J. G. McInerney, and G. Huyet, "RF linewidth in monolithic passively mode-locked semiconductor laser," *IEEE Photon. Technol. Lett.* **20**, 1405–1407 (2008).
- E. U. Rafailov, M. A. Cataluna, W. Sibbett, N. D. Il'inskaya, Y. M. Zadiranov, A. E. Zhukov, V. M. Ustinov, D. A. Livshits, A. R. Kovsh, and N. N. Ledentsov, "High-power picosecond and femtosecond pulse generation from a two-section mode-locked quantum-dot laser," *Appl. Phys. Lett.* **87**, 081107 (2005).
- M. G. Thompson, A. Rae, R. L. Sellin, C. Marinelli, R. V. Penty, I. H. White, A. R. Kovsh, S. S. Mikhlin, D. A. Livshits, and I. L. Krestnikov, "Subpicosecond high-power mode locking using flared waveguide monolithic quantum-dot lasers," *Appl. Phys. Lett.* **88**, 133119 (2006).
- M. T. Todaro, J. P. Tourrenc, S. P. Hegarty, C. Kelleher, B. Corbett, G. Huyet, and J. G. McInerney, "Simultaneous achievement of narrow pulse width and low pulse-to-pulse timing jitter in 1.3  $\mu\text{m}$  passively mode-locked quantum-dot lasers," *Opt. Lett.* **31**, 3107–3109 (2006).
- S. Liu, J. C. Norman, D. Jung, M. Kennedy, A. Gossard, and J. E. Bowers, "Monolithic 9 GHz passively mode locked quantum dot lasers directly grown on on-axis (001) Si," *Appl. Phys. Lett.* **113**, 041108 (2018).
- D. Auth, S. Liu, J. Norman, J. Edward Bowers, and S. Breuer, "Passively mode-locked semiconductor quantum dot on silicon laser with 400 Hz RF line width," *Opt. Express* **27**, 27256–27266 (2019).
- S. Liu, X. Wu, D. Jung, J. Norman, M. J. Kennedy, H. Tsang, A. Gossard, and J. Bowers, "High-channel-count 20 GHz passively mode-locked quantum dot laser directly grown on Si with 4.1 Tbit/s transmission capacity," *Optica* **6**, 128–134 (2019).
- G. Liu, Z. Lu, J. Liu, Y. Mao, M. Vachon, C. Song, P. Barrios, and P. J. Poole, "Passively mode-locked quantum dash laser with an aggregate 5.376 Tbit/s PAM-4 transmission capacity," *Opt. Express* **28**, 4587–4593 (2020).
- V. Vujicic, C. Calo, R. Watts, F. Lelarge, C. Browning, K. Merghem, A. Martinez, A. Ramdane, and L. Barry, "Quantum dash mode-locked lasers for data centre applications," *IEEE J. Sel. Top. Quantum Electron.* **21**, 53–60 (2015).
- J. N. Kemal, P. Marin-Palomo, K. Merghem, G. Aubin, C. Calo, R. Brenot, F. Lelarge, A. Martinez, S. Randel, W. Freude, and C. Koos, "Coherent WDM transmission using quantum-dash mode-locked laser diodes as multi-wavelength source and local oscillator," *Opt. Express* **27**, 31164–31175 (2019).
- Z. Lu, J. Liu, C. Song, J. Weber, Y. Mao, S. Chang, H. Ding, P. Poole, P. Barrios, and D. Poitras, "High performance InAs/InP quantum dot 34.462-GHz C-band coherent comb laser module," *Opt. Express* **26**, 2160–2167 (2018).
- Y. Arakawa and H. Sakaki, "Multidimensional quantum well laser and temperature dependence of its threshold current," *Appl. Phys. Lett.* **40**, 939–941 (1982).
- K. Nishi, K. Takemasa, M. Sugawara, and Y. Arakawa, "Development of quantum dot lasers for data-com and silicon photonics applications," *IEEE J. Sel. Top. Quantum Electron.* **23**, 1901007 (2017).
- M. A. Cataluna, W. Sibbett, D. A. Livshits, J. Weimert, A. R. Kovsh, and E. U. Rafailov, "Stable mode-locked operation up to 80°C from an InGaAs quantum-dot laser," *Appl. Phys. Lett.* **89**, 1500–1502 (2006).
- J. K. Mee, M. T. Crowley, N. Patel, D. Murrell, R. Raghunathan, A. Aboketaf, A. Elshaari, S. F. Preble, P. Ampadu, and L. F. Lester, "A passively mode-locked quantum-dot laser operating over a broad temperature range," *Appl. Phys. Lett.* **101**, 071112 (2012).
- M. Laemmlin, G. Fiol, C. Meuer, M. Kuntz, F. Hopfer, A. R. Kovsh, N. N. Ledentsov, and D. Bimberg, "Distortion-free optical amplification of 20–80 GHz modelocked laser pulses at 1.3  $\mu\text{m}$  using quantum dots," *Electron. Lett.* **42**, 697–699 (2006).
- K. Nishi, T. Kageyama, M. Yamaguchi, Y. Maeda, K. Takemasa, T. Yamamoto, M. Sugawara, and Y. Arakawa, "Molecular beam epitaxial growths of high-optical-gain InAs quantum dots on GaAs for long-wavelength emission," *J. Cryst. Growth* **378**, 459–462 (2013).
- K. A. Williams, M. G. Thompson, and I. H. White, "Long-wavelength monolithic mode-locked diode lasers," *New J. Phys.* **6**, 179 (2004).
- J. O'Gorman, A. F. J. Levi, T. Tanbun-Ek, and R. A. Logan, "Saturable absorption in intracavity loss modulated quantum well lasers," *Appl. Phys. Lett.* **59**, 16–18 (1991).
- J. K. Mee, M. T. Crowley, D. Murrell, R. Raghunathan, and F. Lester, "Temperature performance of monolithic passively mode-locked quantum dot lasers: experiments and analytical modeling," *IEEE J. Sel. Top. Quantum Electron.* **19**, 1101110 (2013).
- F. Klopf, S. Deubert, J. P. Reithmaier, and A. Forchel, "Correlation between the gain profile and the temperature-induced shift in wavelength of quantum-dot lasers," *Appl. Phys. Lett.* **81**, 217–219 (2002).
- L. Li, M. Rossetti, A. Fiore, L. Occhi, and C. Velez, "Wide emission spectrum from superluminescent diodes with chirped quantum dot multi-layers," *Electron. Lett.* **41**, 41–43 (2005).
- K. Zhou, Q. Jiang, Z. Zhang, S. Chen, H. Liu, Z. Lu, K. Kennedy, S. Matcher, and R. Hogg, "Quantum dot selective area intermixing for broadband light sources," *Opt. Express* **20**, 26950–26957 (2012).
- S. Chen, W. Li, Z. Zhang, D. Childs, K. Zhou, J. Orchard, K. Kennedy, M. Hugues, E. Clarke, I. Ross, O. Wada, and R. Hogg, "GaAs-based superluminescent light-emitting diodes with 290-nm emission bandwidth by using hybrid quantum well/quantum dot structures," *Nanoscale Res. Lett.* **10**, 340 (2015).